Electronic Supplementary Information for

Carbon Dioxide in the Cage: Manganese Metal-Organic Frameworks for High Performance CO_2 Electrodes in Li-CO_2 Batteries

Siwu Li, Yu Dong, Junwen Zhou,* Yuan Liu, Jiaming Wang, Xing Gao, Yuzhen Han, Pengfei Qi, and Bo Wang*

Beijing Key Laboratory of Photoelectronic/Electrophotonic Conversion Materials, Key Laboratory of Cluster Science, Ministry of Education, School of Chemistry and Chemical Engineering, Beijing Institute of Technology, Beijing 100081, P. R. China

E-mails: frostfire@sina.com (J.Z); bowang@bit.edu.cn (B.W)

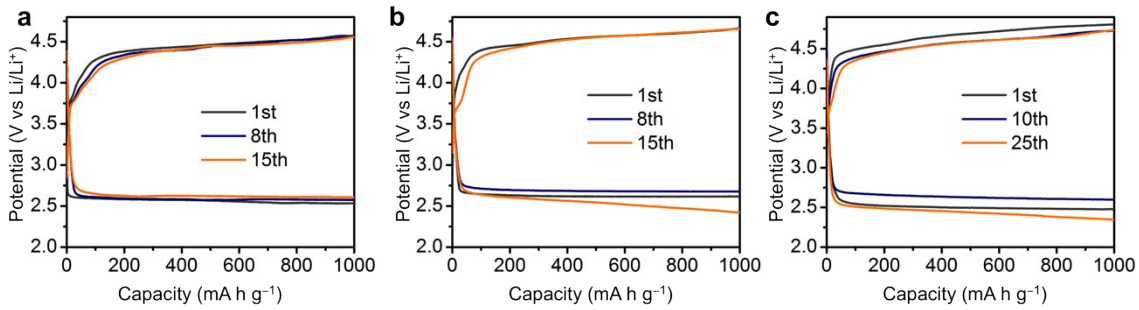

Fig. S1 Discharge-charge voltage curves of CNT electrodes cycled at (a) 50 mA g^{-1}, (b) 100 mA g^{-1}, and (c) 200 mA g^{-1} with a capacity limit of 1000 mA h g^{-1}.

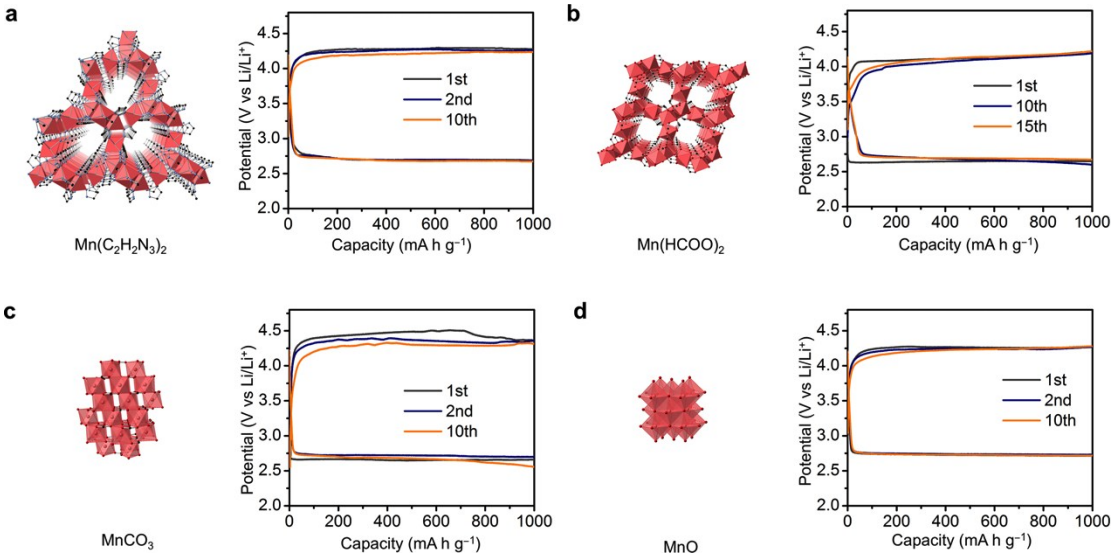

Fig. S2 Crystal structures of (a) $Mn(C_2H_2N_3)_2$, (b) $Mn(HCOO)_2$, (c) $MnCO_3$ and (d) MnO (left) and their corresponding discharge-charge voltage curves at 50 mA g^{-1} with a capacity limit of 1000 mA h g^{-1} (right).

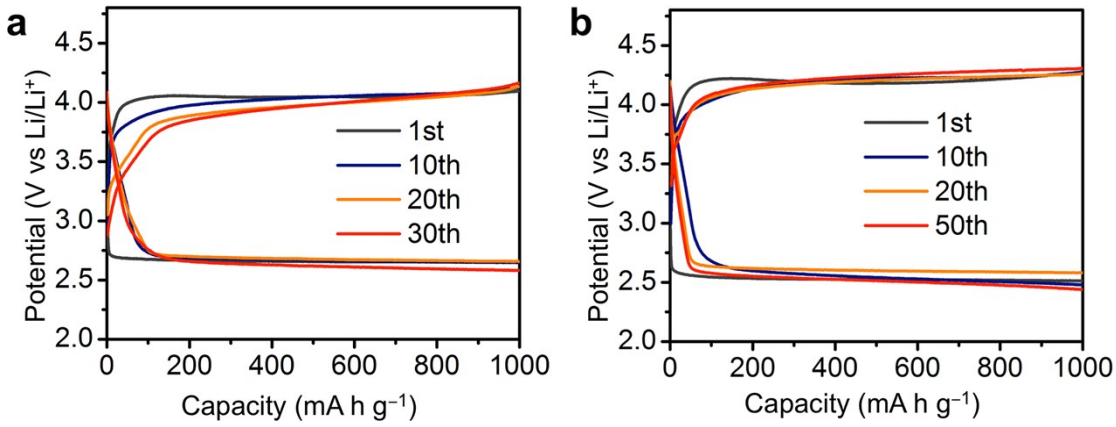

Fig. S3 Discharge-charge voltage curves of Mn_2(dobdc) electrodes cycled at (a) 100 mA g^{-1} and (b) 200 mA g^{-1} with a capacity limit of 1000 mA h g^{-1}.

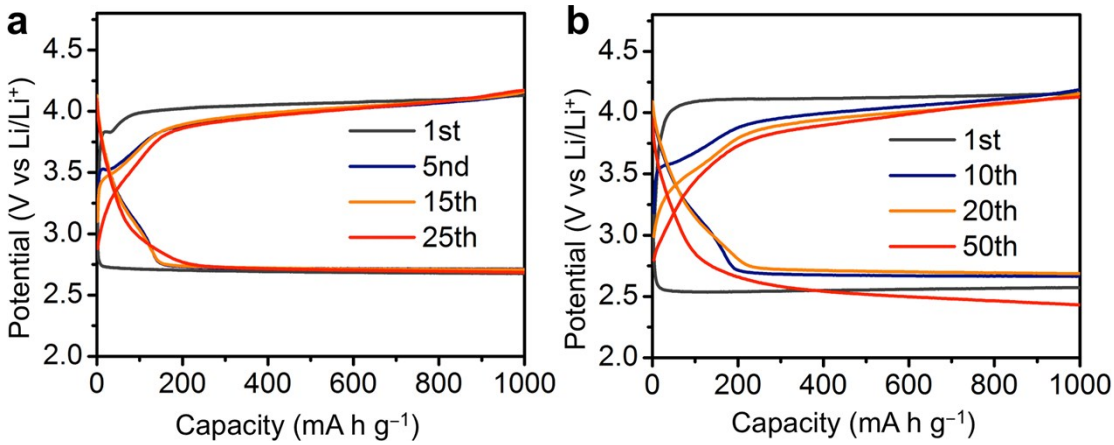

Fig. S4 Discharge-charge voltage curves of $Mn(HCOO)_2$ electrodes cycled at (a) 100 mA g^{-1} and (b) 200 mA g^{-1} with a capacity limit of 1000 mA h g^{-1}.

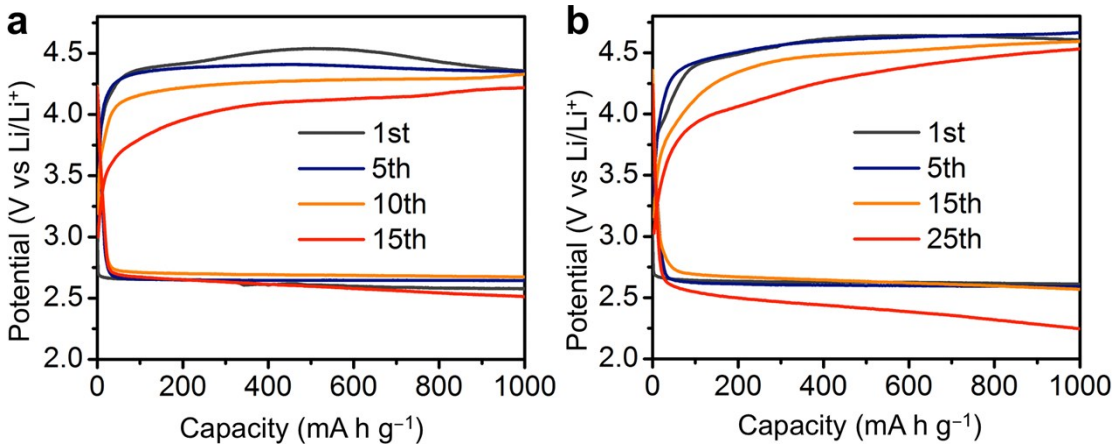

Fig. S5 Discharge-charge voltage curves of $MnCO_3$ electrodes cycled at (a) 100 mA g^{-1} and (b) 200 mA g^{-1} with a capacity limit of 1000 mA h g^{-1}.

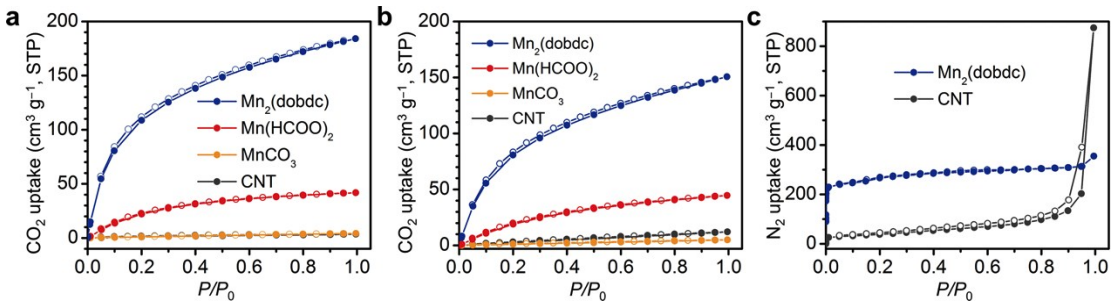

Fig. S6 CO_2 adsorption isotherms of $Mn_2(dobdc)$, $Mn(HCOO)_2$, $MnCO_3$ and CNT at (a) 273 K and (b) 283 K. (c) N_2 adsorption isotherms of $Mn_2(dobdc)$ and CNT at 77 K.

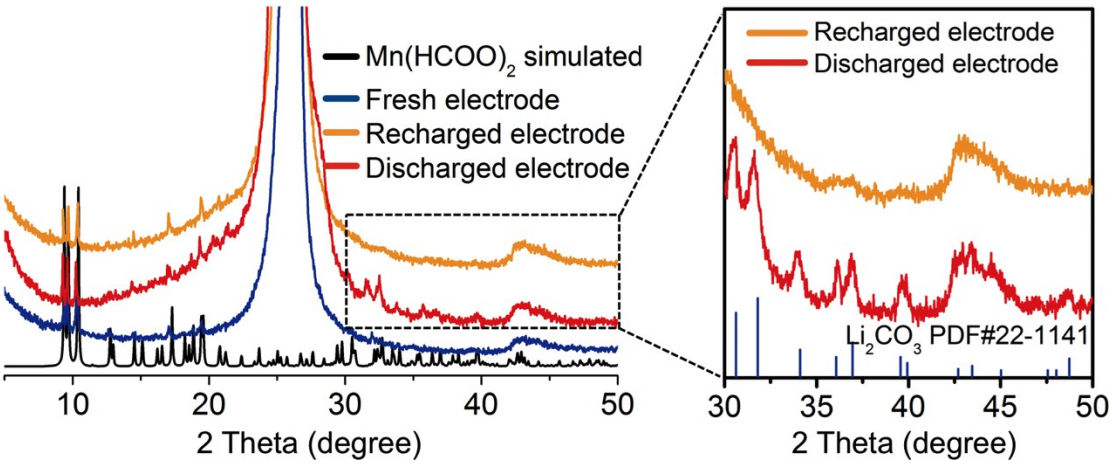

Fig. S7 PXRD patterns of a fresh, a discharged and a recharged $Mn(HCOO)_2$ electrode. The cells were operated at 50 mA g^{-1} with a capacity limit of 1000 mA h g^{-1}. The enlarged figure highlights the formation and decomposition of Li_2CO_3.

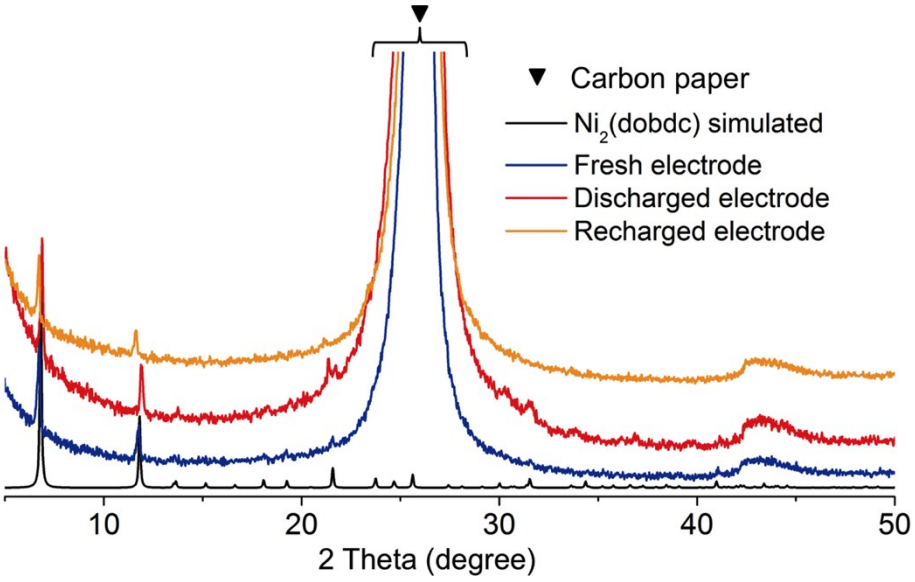

Fig. S8 PXRD patterns of a fresh, a discharged and a recharged Ni_2(dobdc) electrode. The cells were operated at 50 mA g^{-1} with a capacity limit of 1000 mA h g^{-1}.

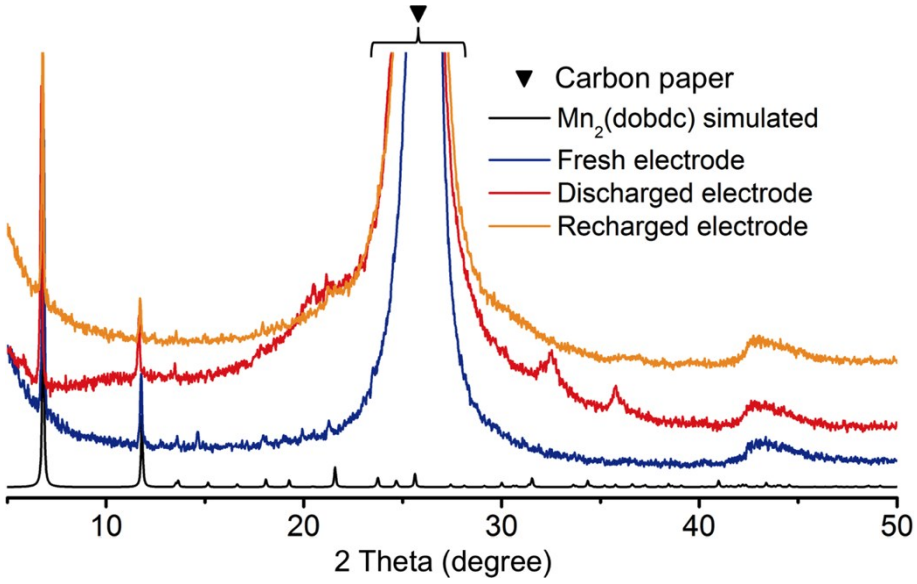

Fig. S9 PXRD patterns of a fresh, a discharged and a recharged Mn_2(dobdc) electrode. The cells were operated at 50 mA g^{-1} with a capacity limit of 1000 mA h g^{-1}.

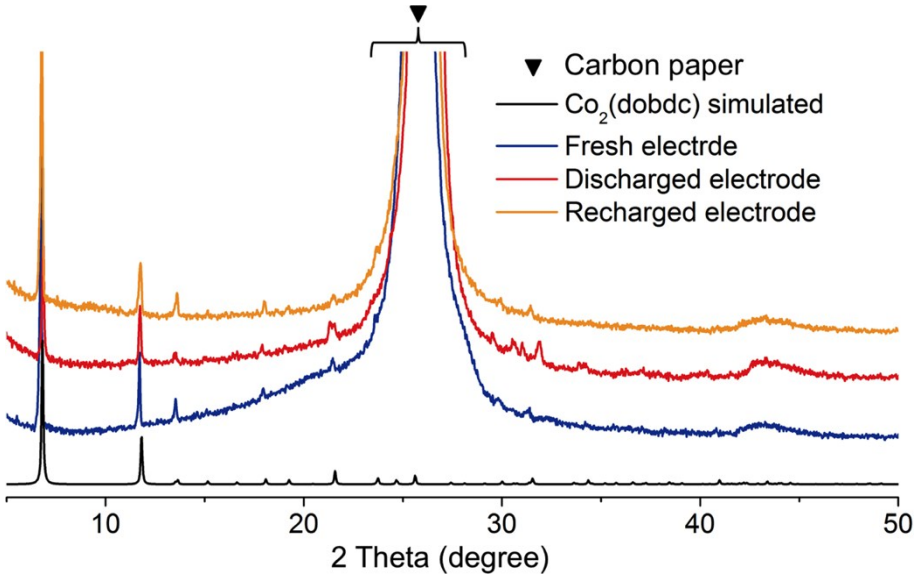

Fig. S10 PXRD patterns of a fresh, a discharged and a recharged Co_2(dobdc) electrode. The cells were operated at 50 mA g^{-1} with a capacity limit of 1000 mA h g^{-1}.

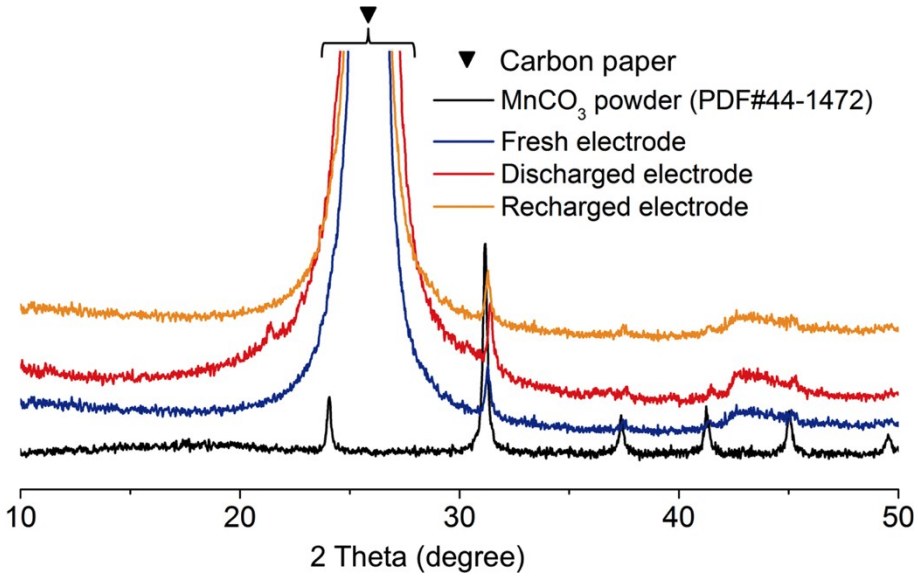

Fig. S11 PXRD patterns of a fresh, a discharged and a recharged $MnCO_3$ electrode. The cells were operated at 50 mA g^{-1} with a capacity limit of 1000 mA h g^{-1}.

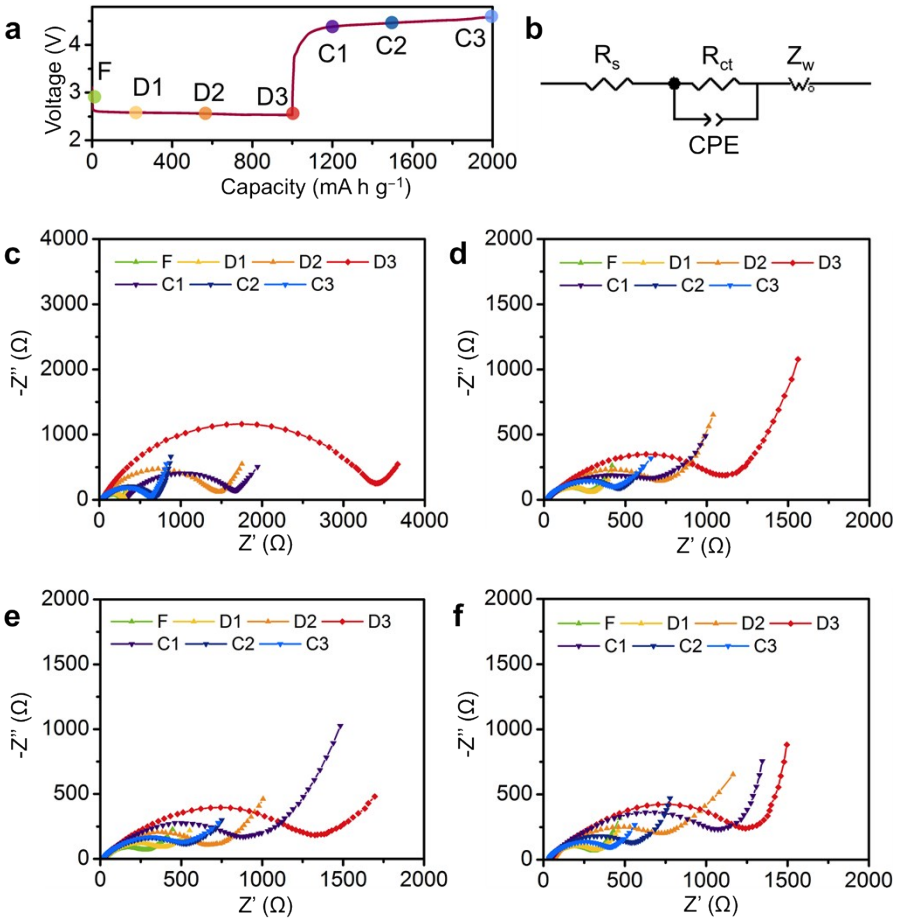

Fig. S12 (a) Typical discharge-charge voltage curves with plots showing the capacity at which an EIS experiment was conducted. (b) Equivalent circuit model for fitting the Nyquist plots. Nyquist plots of (c) CNT, (d) Mn_2(dobdc), (e) $Mn(HCOO)_2$, and (f) $MnCO_3$ electrodes at different discharge and charge states (F: fresh electrode; D1-D3: discharged to 200, 500 and 1000 mA h g^{-1}, respectively; C1-C3: recharged to 200, 500 and 1000 mA h g^{-1}, respectively).

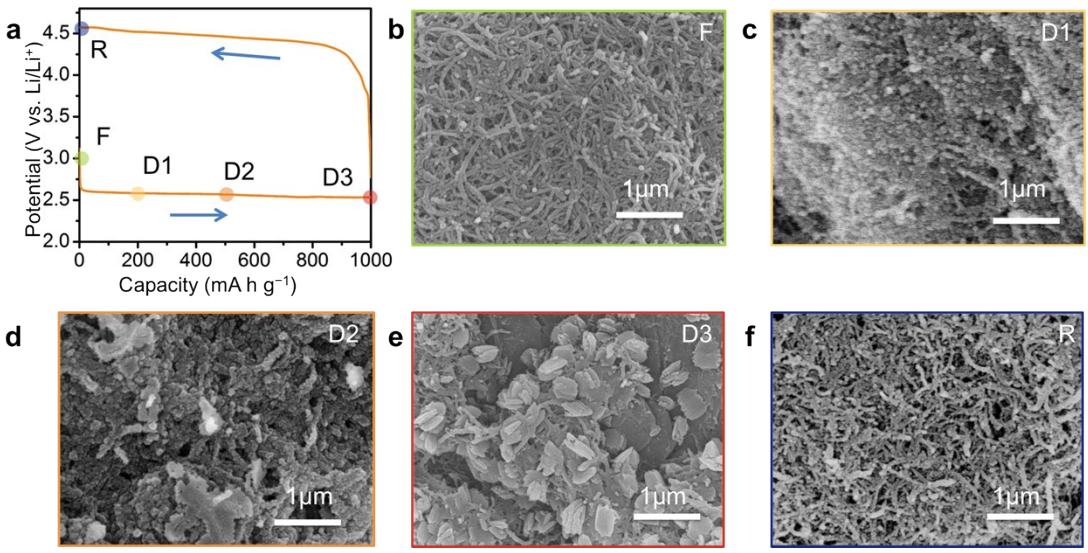

Fig. S13 (a) Discharge-charge voltage curves of a CNT electrode. (b-f) SEM images of CNT electrodes at different states during operation at 50 mA g^{-1} (F: fresh electrode; D1-D3: discharged to 200, 500 and 1000 mA h g^{-1}, respectively; R: recharged to 1000 mA h g^{-1}).

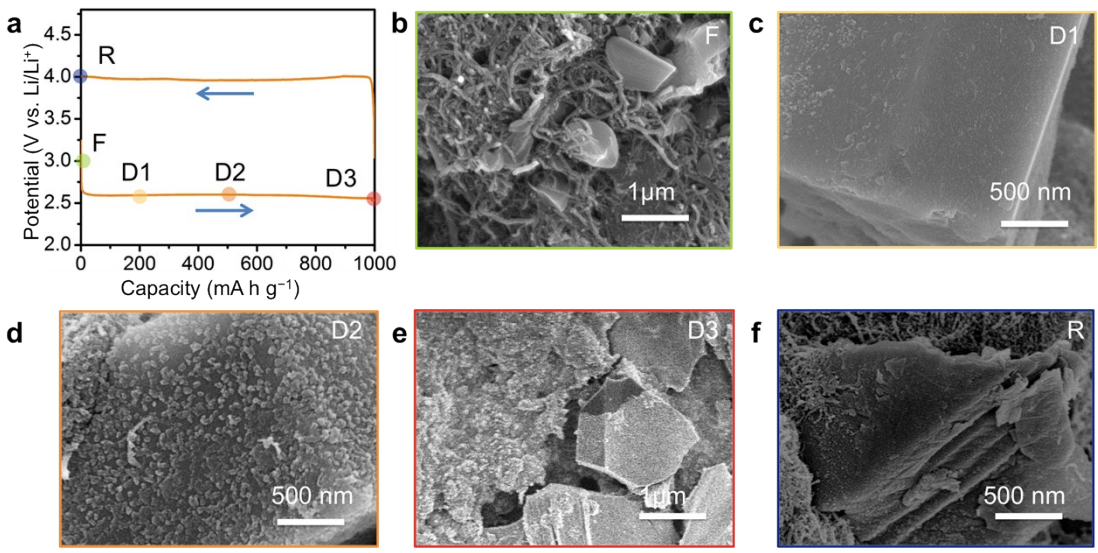

Fig. S14 (a) Discharge-charge voltage curves of a Mn_2(dobdc) electrode. (b-f) SEM images of Mn_2(dobdc) electrodes at different states during operation at 50 mA g^{-1} (F: fresh electrode; D1-D3: discharged to 200, 500 and 1000 mA h g^{-1}, respectively; R: recharged to 1000 mA h g^{-1}).

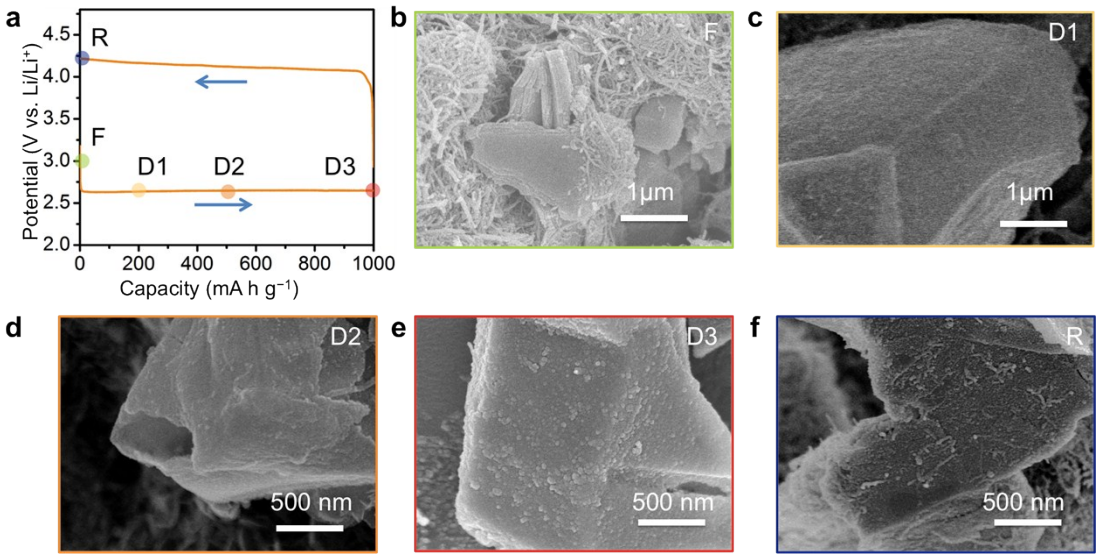

Fig. S15 (a) Discharge-charge voltage curves of a $Mn(HCOO)_2$ electrode. (b-f) SEM images of $Mn(HCOO)_2$ electrodes at different states during operation at 50 mA g^{-1} (F: fresh electrode; D1-D3: discharged to 200, 500 and 1000 mA h g^{-1}, respectively; R: recharged to 1000 mA h g^{-1}).

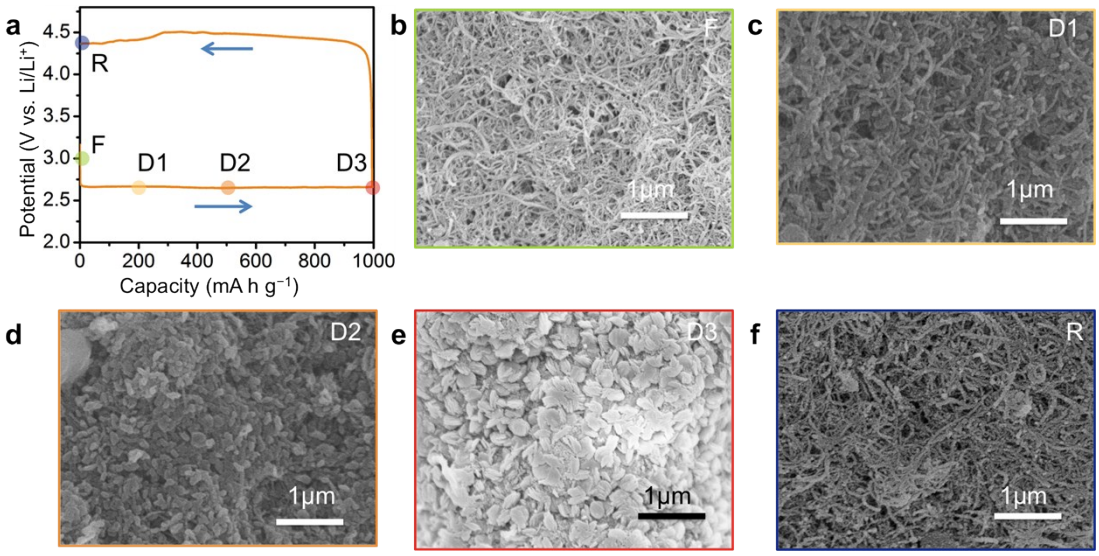

Fig. S16 (a) Discharge-charge voltage curves of a $MnCO_3$ electrode. (b-f) SEM images of $MnCO_3$ electrodes at different states during operation at 50 mA g^{-1} (F: fresh electrode; D1-D3: discharged to 200, 500 and 1000 mA h g^{-1}, respectively; R: recharged to 1000 mA h g^{-1}).

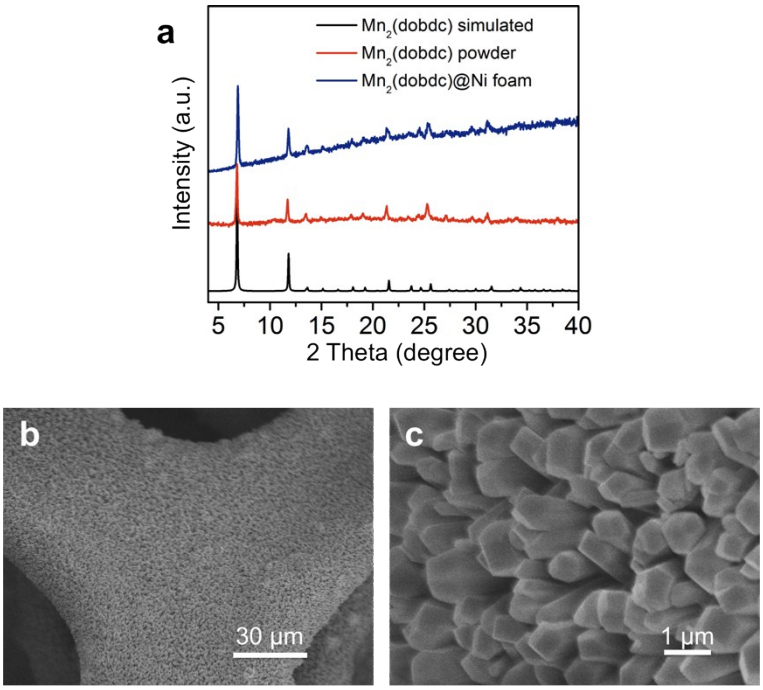

Fig. S17 (a) PXRD patterns, (b) and (c) SEM images of Mn_2(dobdc)@Ni foam.

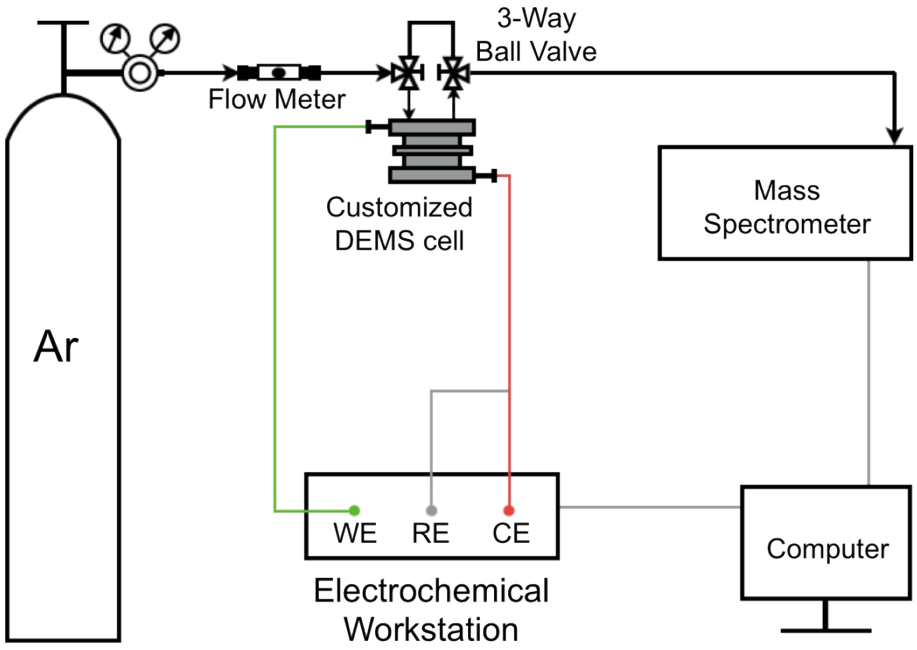

Fig. S18 Schematics of the DEMS system.

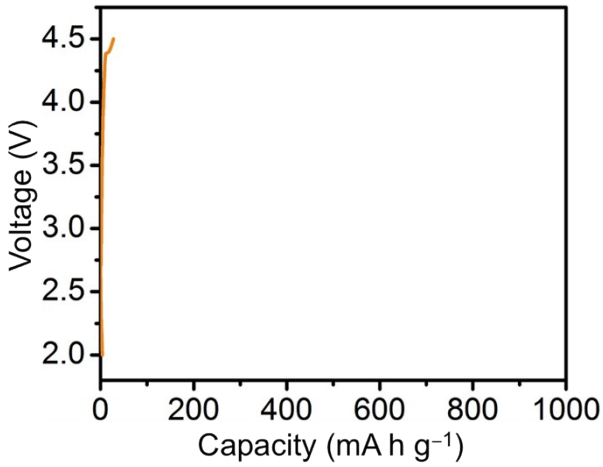

Fig. S19 Discharge-charge voltage curves of a Mn_2(dobdc) electrode tested in Ar atmosphere at 50 mA g^{-1}.

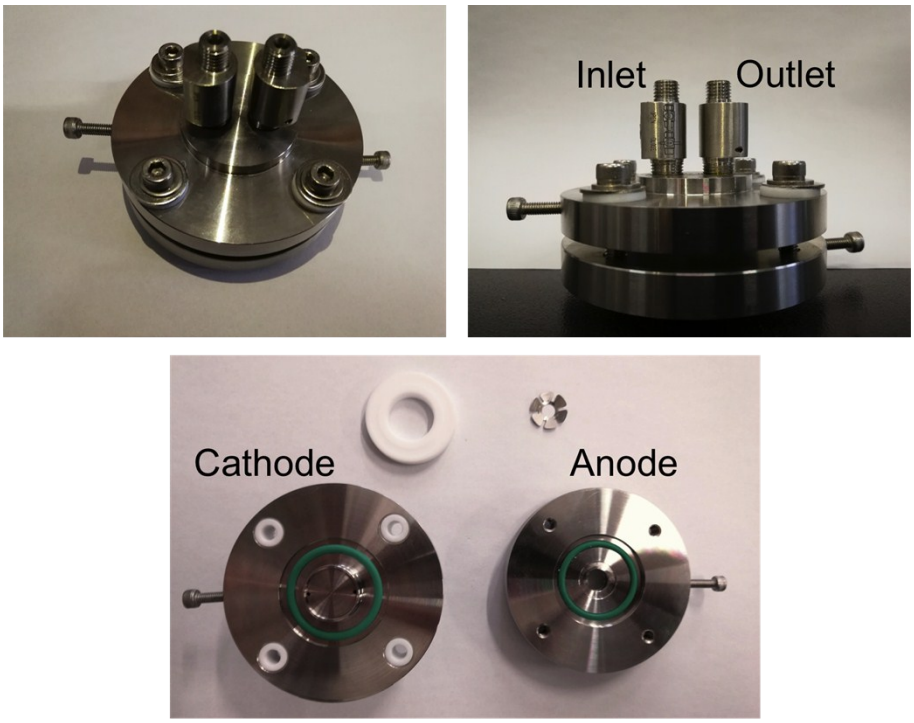

Fig. S20 Photographs of a customized Swagelok cell for *in situ* DEMS.

Table S1. Summary of performance of existing CO_2 electrodes working in pure CO_2.

CO_2 electrode	Full discharge capacity (mA h g^{-1})[a]	Average charge potential (V)[b]	Cycle life	Ref.
Mn_2(dobdc)	18022 (50 mA g^{-1})	3.96 (50 mA g^{-1})	50 (200 mA g^{-1})	This work
$Mn(HCOO)_2$	15510 (50 mA g^{-1})	4.00 (100 mA g^{-1})	50 (200 mA g^{-1})	
Ketjen-black	<100 (0.1 mA cm^{-2})	N/A	N/A	1
	1808 (30 mA g^{-1})	4.26 (30 mA g^{-1})	9 (30 mA g^{-1})	2
High surface area carbon	~800 (0.05 mA cm^{-2})	N/A	N/A	3
	~3000 (0.05 mA cm^{-2})[c]	N/A	N/A	
CNTs	8379 (50 mA g^{-1})	4.3 (50 mA g^{-1})	29 (50 mA g^{-1})	4
Graphene	14774 (50 mA g^{-1})	4.07 (50 mA g^{-1})	20 (50 mA g^{-1})	5
B,N-codoped holey graphene	16033 (300 mA g^{-1})	3.97 (100 mA g^{-1})	200 (1000 mA g^{-1})	6
Ru@Super P	8229 (100 mA g^{-1})	3.93 (100 mA g^{-1})	70 (100 mA g^{-1})	7
Mo_2C@CNT[d]	~360 (~5 mA g^{-1})	~3.5 (~5 mA g^{-1})	40 (~5 mA g^{-1})	8
Ni-NG	17625 (100 mA g^{-1})	4.2 (100 mA g^{-1})	101 (100 mA g^{-1})	9

[a] Full discharge capacity is the discharge capacity toward a cutoff potential of 2.0 V under the given current density. All the capacity and current density values, unless specified otherwise, are normalized by the total mass of catalyst and conductive agent.

[b] Average charge potential is the average of potential during a charge process with a capacity limit of 1000 mA h g^{-1}.

[c] This value was obtained at 100 °C.

[d] The capacity and current density values of Mo_2C@CNT are calculated based on the loading mass of 4 mg on the electrode. The capacity limit for deriving the average charge potential is ~30 mA h g^{-1}.

Table S2. Charge transfer resistance (R_{ct}) of different CO_2 electrodes at different discharge and charge states (Fitting results of **Fig. S12**).

CO_2 electrode	R_{ct} (Ω)						
	F	D1	D2	D3	C1	C2	C3
CNT	276	295	1474	3397	1667	683	623
Mn_2(dobdc)	279	291	712	1115	650	458	434
$Mn(HCOO)_2$	281	383	672	1326	881	535	507
$MnCO_3$	308	329	745	1241	1072	542	414

F: fresh electrode; D1-D3: discharged to 200, 500 and 1000 mA h g^{-1}, respectively; C1-C3: recharged to 200, 500 and 1000 mA h g^{-1}, respectively.

References

(1) Takechi, K.; Shiga, T.; Asaoka, T. *Chem. Commun.* **2011,** *47* (12), 3463.

(2) Liu, Y.; Wang, R.; Lyu, Y.; Li, H.; Chen, L. *Energy Environ. Sci.* **2014,** *7* (2), 677.

(3) Xu, S. M.; Das, S. K.; Archer, L. A. *RSC Adv.* **2013,** *3* (18), 6656.

(4) Zhang, X.; Zhang, Q.; Zhang, Z.; Chen, Y.; Xie, Z.; Wei, J.; Zhou, Z. *Chem. Commun.* **2015,** *51* (78), 14636.

(5) Zhang, Z.; Zhang, Q.; Chen, Y.; Bao, J.; Zhou, X.; Xie, Z.; Wei, J.; Zhou, Z. *Angew. Chem. Int. Ed.* **2015,** *54* (22), 6550.

(6) Qie, L.; Lin, Y.; Connell, J. W.; Xu, J.; Dai, L. *Angew. Chem. Int. Ed.* **2017,** *56*, 1.

(7) Yang, S.; Qiao, Y.; He, P.; Liu, Y.; Cheng, Z.; Zhu, J.; Zhou, H. *Energy Environ. Sci.* **2017,** *10* (4), 972.

(8) Hou, Y.; Wang, J.; Liu, L.; Liu, Y.; Chou, S.; Shi, D.; Liu, H.; Wu, Y.; Zhang, W.; Chen, J. *Adv. Funct. Mater.* **2017**, 1700564.

(9) Zhang, Z.; Wang, X.-G.; Zhang, X.; Xie, Z.; Chen, Y.-N.; Ma, L.; Peng, Z.; Zhou, Z. *Adv. Sci.* **2017**, 1700567.